ESC European Society of Cardiology

European Heart Journal - Cardiovascular Imaging (2021) **00**, 1–8
doi:10.1093/ehjci/jeab009

Blood flow characteristics after aortic valve neocuspidization in paediatric patients: a comparison with the Ross procedure

Aurelio Secinaro [1]*, Elena Giulia Milano[2,3], Paolo Ciancarella[1], Matteo Trezzi[4], Claudio Capelli[2], Paolo Ciliberti[4], Enrico Cetrano[4], Davide Curione[1], Teresa Pia Santangelo[1], Carmela Napolitano[1], Sonia B. Albanese[4], and Adriano Carotti[4]

[1]Advanced Cardiovascular Imaging Unit, Department of Imaging, Bambino Gesù Children's Hospital, IRCCS, Piazza S. Onofrio 4, 00165 Rome, Italy; [2]University College London, Institute of Cardiovascular Science, London, UK; [3]Great Ormond Street Hospital for Children, Department of Cardiology, London, UK; and [4]Department of Pediatric Cardiology and Cardiac Surgery, Bambino Gesù Children's Hospital, IRCCS, Rome, Italy

Received 4 May 2021; accepted 13 January 2021

Aims The aortic valve (AV) neocuspidization (Ozaki procedure) is a novel surgical technique for AV disease that preserves the natural motion and cardiodynamics of the aortic root. In this study, we sought to evaluate, by 4D-flow magnetic resonance imaging, the aortic blood flow characteristics after AV neocuspidization in paediatric patients.

Methods and results Aortic root and ascending aorta haemodynamics were evaluated in a population of patients treated with the Ozaki procedure; results were compared with those of a group of patients operated with the Ross technique. Cardiovascular magnetic resonance studies were performed at 1.5 T using a 4D flow-sensitive sequence acquired with retrospective electrocardiogram-gating and respiratory navigator. Post-processing of 4D-flow analysis was performed to calculate flow eccentricity and wall shear stress. Twenty children were included in this study, 10 after Ozaki and 10 after Ross procedure. Median age at surgery was 10.7 years (range 3.9–16.5 years). No significant differences were observed in wall shear stress values measured at the level of the proximal ascending aorta between the two groups. The analysis of flow patterns showed no clear association between eccentric flow and the procedure performed. The Ozaki group showed just a slightly increased transvalvular maximum velocity.

Conclusion Proximal aorta flow dynamics of children treated with the Ozaki and the Ross procedure are comparable. Similarly to the Ross, Ozaki technique restores a physiological laminar flow pattern in the short-term follow-up, with the advantage of not inducing a bivalvular disease, although further studies are warranted to evaluate its long-term results.

Keywords magnetic resonance imaging • aortic valve disease • bicuspid aortic valve • aortic valve repair • 4D flow

Introduction

The optimal management of aortic valve (AV) disease in children is still challenging. If AV replacement (AVR) is indicated, four main types of AV substitutes are generally considered: pulmonary autografts (i.e. Ross procedure), mechanical, biological valve prostheses, or homografts.[1] Although each option has specific advantages and drawbacks,[2] the Ross operation, first reported in 1967,[3] currently represents the preferred procedure in children with severe AV dysfunction.[4,5] However, concerns regarding autograft dilatation and durability of

* Corresponding author. Tel: +39 (06) 6859 2792; Fax: +39 (06) 6859 2394. E-mail: aurelio.secinaro@opbg.net

both autograft and pulmonary conduit are far from negligible, suggesting a growing need for development of alternative solutions.[6] In this scenario, there is a rising interest in AV neocuspidization (AV Neo) according to the technique described by Ozaki,[7] which showed satisfactory freedom from reoperation at follow-up in an adult population.[8] The use of the Ozaki technique in children, as an alternative to the Ross technique, has shown promising results[9], but it is burdened by limited follow-up and haemodynamic profile data.[10,11]

Aortic blood flow visualization and quantification throughout the cardiac cycle has recently been studied by 4D-flow cardiovascular magnetic resonance (CMR) in both congenital and acquired heart disease, such as bicuspid AV (BAV),[12] ascending aorta (AAo) dilatation,[13] and aortic coarctation.[14] Specifically, in AV disease asymmetrical leaflet opening causes abnormal rotational flow that hits the aortic wall[15] and is associated with increased wall shear stress and AAo diameters.[12,13]

In Ross patients, 4D-flow CMR studies showed a laminar flow pattern in the AAo,[16] comparable to a physiological haemodynamic profile. On the other hand, there is no data in the literature regarding AV Neo patients.

We, therefore, aimed to study a population of patients undergoing either Ross or AV Neo surgery at our institution to compare the haemodynamic profile following the two procedures. The study was conducted using 4D-flow CMR and haemodynamic assessment included both aortic root and AAo analysis in all patients.

Methods

Study population

Twenty patients who underwent AVR at our institution were prospectively recruited in this study. The study population included a group of 10 consecutive patients who underwent AV Neo (AV Neo group) and a group of 10 Ross patients (Ross group), enrolled for a follow-up CMR study.

The study complied with the declaration of Helsinki and was approved by local ethics committee; written informed consent was obtained for all participants.

Surgical procedures

The Ross operation was mainly performed in patients with AV stenosis, while the AV Neo procedure was implemented regardless of the preponderant anatomic lesion. Briefly, all procedures were performed on moderate hypothermic cardiopulmonary bypass with aortic-bicaval cannulation and cardioplegic cardiac arrest. The Ross operation was carried out by autograft transplantation of native pulmonary root according to a standard full root technique, with coronary reimplantation and allograft reconstruction of the right ventricular outflow tract. The AV Neo procedure was performed using either autologous pericardium when available or decellularized bovine pericardium (CardioCel, Milton, Australia). The details of the surgical technique used for AV Neo have been previously reported.[17]

CMR acquisition protocol

All patients included in this study were prospectively recruited for a follow-up CMR performed on a 1.5 T scanner (MAGNETOM Aera, Siemens Healthcare, Erlangen, Germany) with a 32-channel cardiac coil. Image acquisition settings and protocols were uniform throughout the study. CMR protocol included conventional retrospectively electrocardiogram (ECG)-gated, breath-held balanced steady-state free precession (bSSFP) cine sequences acquired in standard cardiac planes (long-axis views and short-axis stack) to quantify left ventricular volumes and function as well as in dedicated AV and aortic root planes to evaluate leaflet excursion. Post-contrast ECG-gated 3D-bSSFP magnetic resonance angiography (MRA) encompassing the whole thoracic aorta and triggered in mid-to-late diastole was obtained in the sagittal plane to measure aortic diameters.

A prototype 4D-flow gradient-echo sequence (3D time-resolved phase-contrast imaging with 3D velocity encoding) was acquired with retrospective ECG-gating during free-breathing, using a respiratory navigator placed at the lung–liver interface. The image acquisition volume was obtained in the sagittal plane encompassing the whole thoracic aorta. Technical parameters were as following: isotropic voxel size ranging from 2.4 to 2.8 mm, field-of-view (FOV) read: 360–380 mm, FOV phase: 68.8–75%, matrix: 128 × 128 or 160 × 160, repetition time: 38 ms, echo time: 2.3 ms, flip angle: 7°, receiver bandwidth 496 Hz/pixel, parallel imaging (GRAPPA) along the phase encoding direction with a reduction factor $R = 2$ or 3. In order to optimize the Velocity-to-Noise Ratio (VNR), velocity encoding (VENC) range was determined using the lowest non-aliasing arterial velocity calculated on conventional 2D phase-contrast images. In our population, VENC values ranged between 180 and 400 cm/s depending on the presence and severity of valve acceleration. The sequence was acquired after intravenous contrast administration (Gadoterate meglumine—DOTAREM, Roissy, Guerbet, France) at 0.2 mmol/kg, to improve image quality.

Image processing and analysis

Image processing and analysis were performed with a commercial software (CMR42, Circle Cardiovascular Imaging Inc., Calgary, Canada). Left ventricular end-diastolic volume (LVEDV), end-systolic volume (LVESV), end-diastolic mass (LVEDM), and ejection fraction (LVEF) were calculated for each patient from short-axis cine bSSFP images. Papillary muscles and trabeculae were included in the blood pool. LVEDV, LVESV, and LVEDM were indexed for body surface area (BSA), calculated with the Mosteller formula.

Aortic measurements were obtained from 3D-bSSFP MRA images: the diameter of the sinuses of Valsalva was the maximal value among the three sinus-to-sinus measurements, the mid-AAo diameter was the maximal value between two orthogonal measurements in a cross-sectional plane at the level of pulmonary bifurcation. All the aortic measurements were traced from inner edge to inner edge of the vessel wall.

Pre-processing correction strategies were applied to all 4D-flow datasets in order to reduce phase offset errors and image noise. Moreover, data quality evaluation was performed to confirm measurement accuracy according to the literature,[18] with quantitative comparison of 4D results and standard 2D phase-contrast sequences. Four-dimensional flow datasets were processed to generate 3D interactive images of blood flowing through the thoracic aorta, visualized as Doppler-like colour-coded streamlines and velocity vectors. After initial segmentation of the region of interest (from the left ventricular outflow tract to the mid-descending aorta), the vessel centreline was automatically computed and manually adjusted when needed. Two reference planes perpendicular to the vessel centreline were identified at the sinotubular junction (P1) and where the mid-AAo crosses the pulmonary bifurcation (P2). These landmarks were used to measure conventional flow and velocity parameters: forward flow (FF), backward flow (BF), net flow (NF), regurgitation fraction (RF), and maximum velocity (Vmax). Flow eccentricity index and wall shear stress were analysed at the same levels. Blood flow eccentricity was evaluated on 2D colour-coded velocity maps obtained in systole, and semi-quantitatively graded by two operators (E.M. and P.C.) as central (Grade

0), mildly eccentric (Grade 1), or markedly eccentric (Grade 2) as previously described in the literature[19,20] (*Figure 1*). Wall shear stress (WSS, unit N/m^2) is a time-resolved 3D force obtained from 4D-flow datasets and calculated as axial, circumferential, and global components (*Figure 1*).

Echocardiography

All patients underwent complete transthoracic echocardiography (Echo) on the same day of the CMR examination. Echo investigations were performed using an Epiq7 or iE33 ultrasound system (Philips Healthcare Inc., Andover, MA, USA). Standard analysis was performed to obtain LV outflow velocities at the level of the 'neo-aorta', using continuous wave Doppler signals from the apical or right parasternal views, and measuring peak/mean gradient and peak velocity. Aortic regurgitation, if present, was evaluated with vena contracta jet width measurement and graded accordingly.[21]

Statistical analysis

Data analysis was performed using MedCalc ver. 15.8 (MedCalc software bvba). For statistical analysis, the Wilcoxon signed-rank test, the Mann–Whitney *U*, and ANOVA test were used. A *P*-value <0.05 was considered to be significant. Values are presented as mean ± standard deviation (SD) or median and range, as appropriate.

Results

Aortic valvulopathy at the time of surgery was in most cases a congenital lesion, with BAV as the predominant diagnosis (65%). Other diagnoses included isolated valvulopathy on a normal three-leaflet valve, truncus arteriosus, rheumatic disease, and valvulopathy associated with subaortic ventricular septal defect. The baseline characteristics of patients are summarized in *Table 1*.

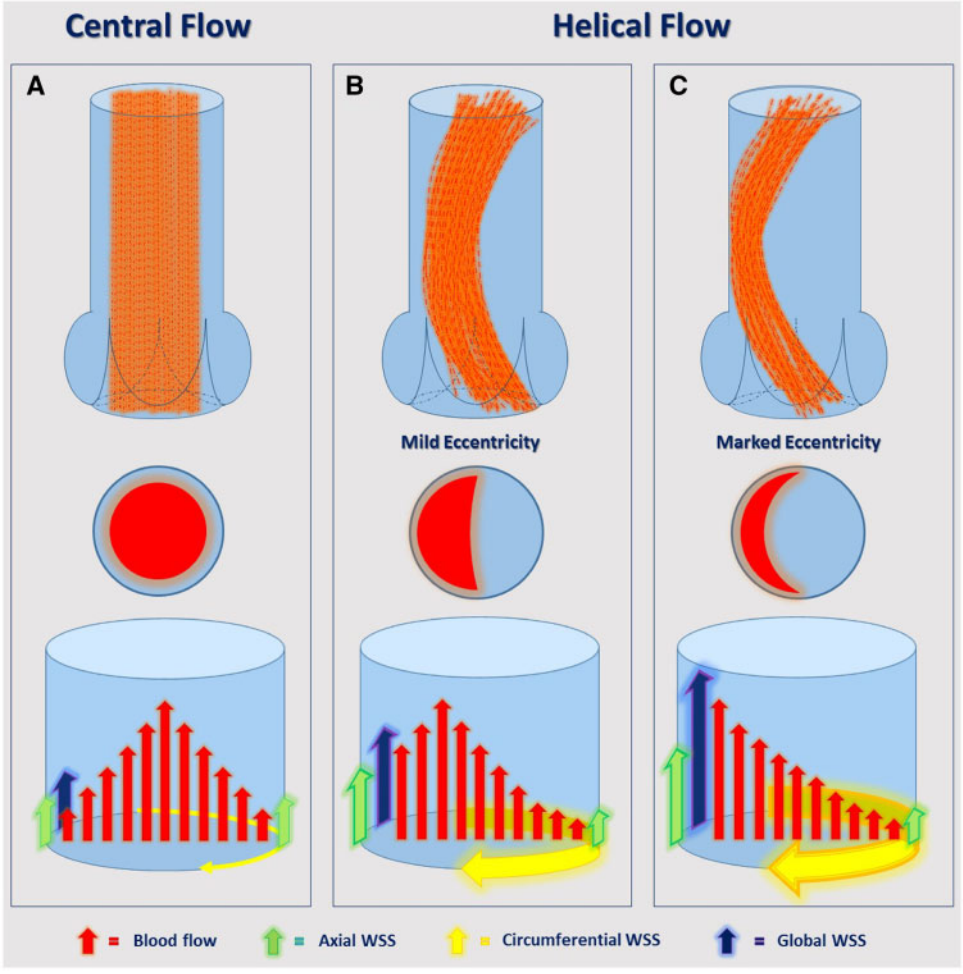

Figure 1 Wall shear stress in the ascending aorta. Different flow and wall shear stress patterns at the level of the ascending aorta. In central flow, high linear systolic flow is focused at the centre and occupies the majority of the vessel lumen; axial WSS represents the main wall shear stress vector of global WSS (*A*). In helical flow, the high systolic blood stream vectors are placed eccentrically towards the periphery of the vessel lumen and fill between one- and two-thirds of the vessel lumen (mild eccentricity, *B*) or one-third or less of the vessel lumen (Marked Eccentricity, *C*), with circumferential WSS representing the dominating vector of global WSS.

Table 1 Patients demographics

	Ross ($n = 10$)	AV Neo ($n = 10$)	*P*-value
Female (%)	1 (10%)	4 (40%)	0.12
Aortic valve defect (%)			
Bicuspid aortic valve	6 (60%)	7 (70%)	0.22
Aortic stenosis	8 (80%)	4 (40%)	0.07
Aortic regurgitation	1 (10%)	5 (50%)	0.05
Mixed stenosis/regurgitation	1 (10%)	1 (10%)	1
Age at surgery (years)	10.6 ± 4.2	11.4 ± 3.1	0.64
Age at scan (years)	16.2 ± 7.9	9.6 ± 2.9	0.008*
Time surgery-to-scan (months)	63.8 ± 64	4 ± 2.4	0.0091*
Body weight at scan (kg)	58.8 ± 17.8	47.5 ± 20.0	0.19
BSA at scan (m^2)	1.60 ± 0.33	1.36 ± 0.38	0.15
Aortic root indexed (mm/BSA)	24.2 ± 3.8	18.8 ± 5.6	0.022*
AAo indexed (mm/BSA)	17.0 ± 3.4	18.5 ± 5.0	0.45

Values are expressed as average and standard deviation.
*$P < 0.05$.

Table 2 Functional parameters

	Ross ($n = 10$)	AV Neo ($n = 10$)	*P*-value
LVEDVi (mL/m^2)	91.2 ± 18.8	79.2 ± 14.4	0.12
LVESVi (mL/m^2)	37.6 ± 10.8	31.2 ± 13.4	0.19
LVEF (%)	59 ± 5	61.1 ± 7.2	0.46
CI (L/min/m^2)	3.47 ± 1.01	3.97 ± 1.04	0.29
LVEDMi (g/m^2)	64.7 ± 13.5	71.5 ± 11.1	0.23
Ao RF (%)	10.5 ± 12.7	9.3 ± 4.0	0.77
Ao Vmax (cm/s)	130 ± 33	220 ± 73	0.0024*
Ao Gmax (mmHg)	7.1 ± 3.7	21 ± 13.8	0.0065*
Ao Vmax echo (cm/s)	157 ± 38	203 ± 63	0.06

Values are expressed as average and standard deviation.
*$P < 0.05$.

Data quality check performed on phase-contrast datasets showed consistency of 4D-flow, with no significant discrepancies between 4D and 2D results. In addition, neither gross aliasing nor aberrant streamlines/pathlines were visualized.

Ross procedure group

Median age at surgery was 10.6 years (range 3.9–16.5 years). Indication for the Ross procedure was aortic stenosis ($n = 8$), aortic regurgitation ($n = 1$), or mixed stenosis-regurgitation ($n = 1$). In four patients, a previous operation on the AV had been performed prior to the Ross procedure. Two patients underwent concomitant aortic annulus enlargement (Ross–Konno procedure). CMR examination was performed at a median of 34 months after the operation (range 6–205 months). At follow-up, patients in the Ross group showed normal transvalvular max velocity (130 ± 33 cm/s) and peak gradient (7.0 ± 3.7 mmHg) across the AV (*Table 2*), with mild regurgitation (RF 10.5 ± 12.7%).

Echocardiographic assessment performed at the same time of CMR study, confirmed normal Vmax values in Ross group (157 ± 38 cm/s). On Echo, six patients (60%) showed a trivial jet of aortic regurgitation and four showed mild (30%) to moderate (10%) neo-aortic incompetence.

AV Neo group

Median age at surgery was 11.4 years (range 7.1–15.9 years). Indication for the AV Neo procedure was aortic regurgitation ($n = 5$), aortic stenosis ($n = 4$), or mixed stenosis-regurgitation ($n = 1$). Two patients had previously undergone AV surgery. Patients in the AV Neo group presented smaller aortic root diameters compared to patients in the Ross group. The native aortic annulus was sized intraoperatively and after cusp excision, with a median diameter of 19 mm (range 16–25 mm). Cusp reconstruction was performed with decellularized heterologous pericardium in six cases, while autologous pericardium treated with buffered 0.6% glutaraldehyde solution was used in the other four.

CMR examination was performed at a median of 4 months after the operation (range 1–10 months). At follow-up, patients in the AV Neo group showed slightly increased maximal velocity across the AV (220 ± 73 cm/s) with no significant regurgitation (RF 9.3 ± 4.0%). Echocardiography confirmed mild transvalvular flow acceleration after AV Neo (203 ± 63 cm/s). Six patients (60%) showed no significant aortic regurgitation at Echo, while four patients (40%) showed mild valve incompetence.

Blood flow pattern

The flow pattern analysis of patients who underwent either the Ross or the AV Neo procedure showed no clear association between an eccentric flow pattern and the operation performed ($P = 0.058$ at the sinotubular junction and $P = 0.17$ at the mid-AAo, respectively) (*Figures 2 and 3*).

At the sinotubular junction, Ross patients showed central flow in 40% of cases and mild eccentricity in 60%, while AV Neo patients had

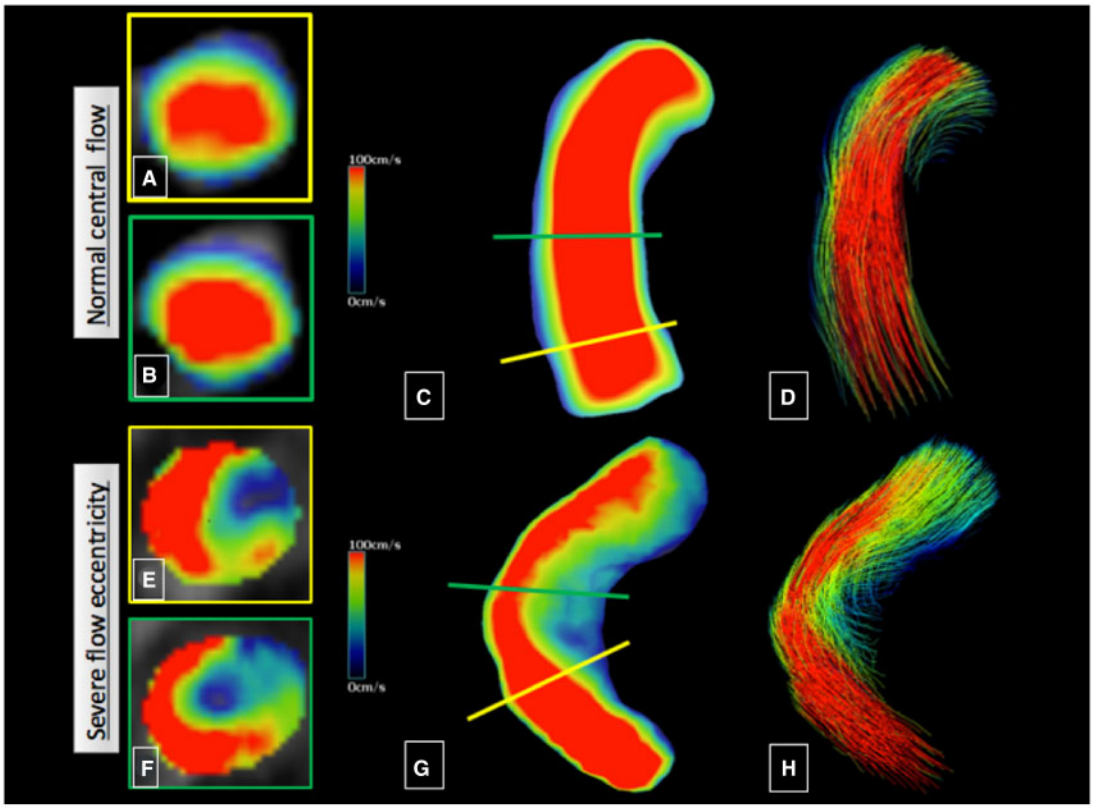

Figure 2 Flow eccentricity. Evaluation of flow eccentricity. Upper panels (*A–D*) show an example of velocity maps of normal central flow at the level of the sinotubular junction (*A*), and mid-ascending aorta (*B*); lower panels (*E–H*) show an example of velocity maps of a case with severe flow eccentricity at the level of the sinotubular junction (*E*), and mid-ascending aorta (*F*).

central flow in 90% of cases and marked eccentricity in 10%, respectively (inter-rater agreement weighted $K = 0.867$). At the mid-AAo, Ross patients showed central flow in 30% of cases and mild eccentricity in 70%, whereas AV Neo patients had central flow in 70% of cases, mild eccentricity in 20%, and marked eccentricity in 10%, respectively (inter-rater agreement Weighted $K = 0.653$) (*Figures 2 and 3*). With regard to the type of material used in the AV Neo group, there were no significant differences between autologous and heterologous pericardium. *Figure 4* and Supplementary data online, *Videos S1 and S2* show aortic fluid dynamics following AV Neo repair.

Wall shear stress

No significant differences were observed in axial, circumferential, and global WSS measured both at the sinotubular junction and mid-AAo between the two groups (*Table 3*). By comparing the type of material used for valve reconstruction, there were no differences between the Ross and AV Neo group as well as between autologous and heterologous pericardium within the AV Neo group (*Table 4*).

Discussion

Although AV repair ideally appears to be the most sensible option in paediatric patients, sometimes it is not feasible or failure occurs, making AVR necessary. Amongst replacement options, the Ross operation has clear advantage over other alternatives, although operative mortality[1,2,4,5,22] and late complications are far from negligible.[6,23,24] Recently, AV Neo has been shown to be a versatile procedure in children with adequate haemodynamic parameters in the short- and medium-term follow-up, despite some concerns raised by the possible use of pericardial substitutes.[25]

In this study, we demonstrated that AV Neo and Ross procedure show similar haemodynamic profiles, analysed by 4D-flow CMR.

The influence of haemodynamic shear stress due to spatial and temporal alterations in shear forces on the endothelium has been described by others, showing regionally different flow and arterial remodelling.[26] The mechanical shear forces induced by blood flow seem to play an important role in the process of valve leaflet injury and vascular remodelling.

Four-dimensional flow CMR has been extensively applied in the *in vivo* investigation of many cardiovascular conditions,[18] historically for research purposes,[12,14] and more recently as a viable clinical tool.[18] Although there is lack of standardization, especially in children, several reports have provided WSS reference values for the thoracic aorta.[27,28] In addition, haemodynamic consequences of aortopathies have been well investigated, even in children.[20,29]

In this study, it was possible to measure and calculate *in vivo* cardiodynamic data in patients who underwent either the Ross or AV Neo procedure.

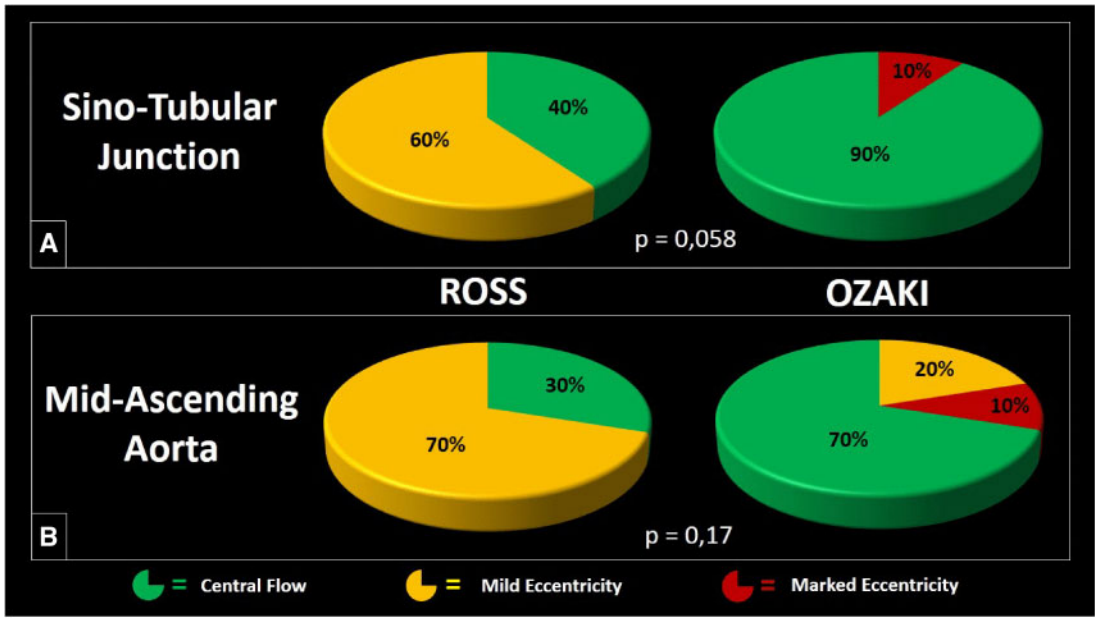

Figure 3 Flow patterns after Ross and AV Neo operations: results of flow evaluation at the level of sinotubular junction (*A*) and mid-ascending aorta (*B*) are shown, with no statistically significant differences found between the two groups.

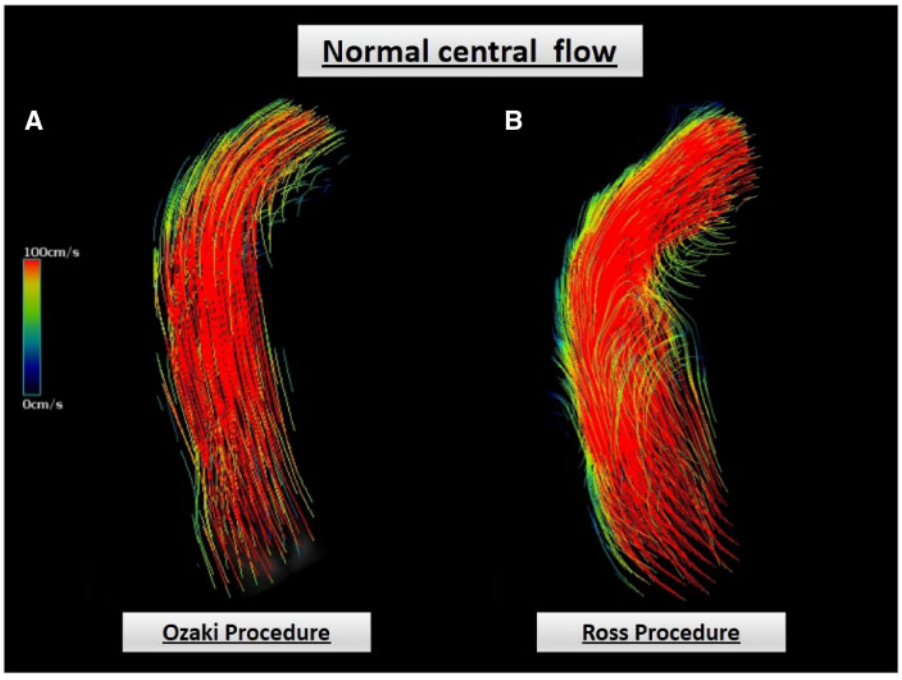

Figure 4 Comparison of ascending aortic 4D flow profiles after AV Neo procedure (*A*) and Ross operation (*B*). Despite an evidence of minor flow turbulences, both Ozaki and Ross procedures are equally able to restore fluid-dynamic conditions very close to normal physiology.

Firstly, we recognized that average Vmax values were higher in the AV Neo group compared to the Ross population, probably related to the smaller indexed aortic root diameters of AV Neo patients. The presence of flow acceleration in the early postoperative period after AV Neo has been previously described.[8] Interestingly, mid-term follow-up confirms that the natural excursion and 'remodelling' of

Table 3 WSS values according to the surgical procedure

	Ross ($n = 10$)	AV Neo ($n = 10$)	*P*-value
Sinotubular junction			
WSS global$_{average}$ (N/m^2)	0.13 ± 0.05	0.16 ± 0.05	0.22
WSS axial$_{average}$ (N/m^2)	0.14 ± 0.04	0.14 ± 0.07	0.93
WSS circ$_{average}$ (N/m^2)	0.07 ± 0.03	0.07 ± 0.02	0.52
Mid-ascending aorta			
WSS global$_{average}$ (N/m^2)	0.13 ± 0.05	0.14 ± 0.04	0.92
WSS axial$_{average}$ (N/m^2)	0.13 ± 0.04	0.12 ± 0.02	0.36
WSS circ$_{average}$ (N/m^2)	0.08 ± 0.02	0.08 ± 0.03	0.74

Values are expressed as average and standard deviation.

Table 4 WSS values according to aortic leaflet tissue

	Ross ($n = 10$)	AV Neo Cardiocell ($n = 6$)	AV Neo Autologus pericardium ($n = 4$)	*P*-value
Sinotubular junction				
WSS global$_{average}$ (N/m^2)	0.13 ± 0.05	0.16 ± 0.05	0.16 ± 0.06	0.48
WSS axial$_{average}$ (N/m^2)	0.13 ± 0.04	0.13 ± 0.03	0.14 ± 0.11	0.90
WSS circ$_{average}$ (N/m^2)	0.07 ± 0.03	0.06 ± 0.02	0.08 ± 0.03	0.33
Mid-ascending aorta				
WSS global$_{average}$ (N/m^2)	0.13 ± 0.05	0.13 ± 0.04	0.15 ± 0.04	0.79
WSS axial$_{average}$ (N/m^2)	0.13 ± 0.04	0.12 ± 0.02	0.11 ± 0.001	0.64
WSS circ$_{average}$ (N/m^2)	0.08 ± 0.02	0.08 ± 0.02	0.09 ± 0.04	0.79

Values are expressed as average and standard deviation.

autologous cusps are distinctive features of the novel technique and they can both contribute to progressive and remarkable improvement of AV Neo haemodynamic compared with conventional AVR. Supporting this statement, blood flow distribution seemed to have a more prominent laminar flow at the sinotubular junction for AV Neo patients, with a *P* value close to statistical significance ($P = 0.058$).

Secondly, despite minor discrepancies among established determinants of theoretical WSS (velocity, vessel diameter, and flow eccentricity), both groups were comparable in terms of aortic WSS. In fact, no significant differences were observed in axial, circumferential, and global WSS measured both at the sinotubular junction and mid-AAo. Although the main fluid-dynamic components were different among the two procedures when considered separately, overall WSS quantification by 4D-flow CMR showed similar haemodynamic performance. Notably, our results suggest that laminar flow and smaller vessel diameters probably balance the higher Vmax in the AV Neo group, while lower flow velocities seem to compensate for larger aortic roots and more prominent eccentric flow in the Ross population.

Finally, when comparing the type of material used for valve reconstruction, in this study no significant differences between autologous pericardium, heterologous pericardium, and autograft tissue in the short-term follow-up were detected, showing comparable haemodynamics within the aortic root and AAo in both AV Neo and Ross groups (*Figure 4*).

Study limitations

This study reports a single-centre experience and has a small sample size. AV Neo group had significantly shorter CMR follow-up time compared to the Ross counterpart. We believe, however, that this discrepancy does not alter the meaning of the study, as it is focused on the flow dynamics and not on the durability of each procedure. In this sense, it was not surprising that the type of material used in the AV Neo group had no influence on the results, contrary to what emerges from studies with more consistent series and follow-up interval of the same institution.[17] We did not include a control group of volunteers in the analysis, as the haemodynamic performance of Ross procedure has been previously compared to normal healthy subjects,[16] considering the Ross procedure as our reference standard. We did not perform inter-observer reproducibility of WSS calculation. However, Van Ooij *et al.*[30] have already investigated the high reproducibility of thoracic 4D-flow parameters for consecutive measurements in healthy controls, with low inter-observer variability.

Finally, future larger multicentre studies with longer follow-up are warranted to confirm these results.

Conclusion

The AV Neo procedure shows similar haemodynamic results in the short-term period compared with the Ross operation. Although slightly higher flow velocities are found in the AAo after AV Neo, both procedures are equally able to restore physiological tri-leaflet fluid-dynamic conditions. The AV Neo technique generates similar short-term haemodynamic results in children needing AVR. The long-term durability of the technique remains to be proven.

Supplementary data

Supplementary data are available at *European Heart Journal - Cardiovascular Imaging* online.

Acknowledgements

We would like to thank the 4D flow 'Work in Progress' sequence developers Daniel Giese (Siemens Healthineers, Germany) and Jin Ning PhD (Siemens Medical Solutions Inc., OH, USA). We are also extremely grateful to the entire group of CMR Radiographers and Nurses operating in the CMR laboratory of Bambino Gesù Children's Hospital.

Funding

CC is supported by the British Heart Foundation project grant PG/17/6/32797.

Data availability

The data underlying this article will be shared on reasonable request to the corresponding author.

Conflict of interest: none declared.

References

1. Akins CW, Miller DC, Turina MI, Kouchoukos NT, Blackstone EH, Grunkemeier GL *et al.* Guidelines for reporting mortality and morbidity after cardiac valve interventions. *Ann Thorac Surg* 2008;**85**:1490–5.
2. Sharabiani MTA, Dorobantu DM, Mahani AS, Turner M, Peter Tometzki AJ, Angelini GD *et al.* Aortic valve replacement and the Ross operation in children and young adults. *J Am Coll Cardiol* 2016;**67**:2858–70.
3. Ross DN. Replacement of aortic and mitral valves with a pulmonary autograft. *Lancet* 1967;**290**:956–8.
4. Elkins RC, Thompson DM, Lane MM, Elkins CC, Peyton MD. Ross operation: 16-year experience. *J Thorac Cardiovasc Surg* 2008;**136**:623–30.e5.
5. Takkenberg JJM, Kappetein AP, Van Herwerden LA, Witsenburg M, Van Osch-Gevers L, Bogers JJC. Pediatric autograft aortic root replacement: a prospective follow-up study. *Ann Thorac Surg* 2005;**80**:1628–33.
6. Etnel JRG, Elmont LC, Ertekin E, Mokhles MM, Heuvelman HJ, Roos-Hesselink JW *et al.* Outcome after aortic valve replacement in children: a systematic review and meta-analysis. *J Thorac Cardiovasc Surg* 2016;**151**:143–52.e3.
7. Ozaki S, Kawase I, Yamashita H, Uchida S, Nozawa Y, Matsuyama T *et al.* Aortic valve reconstruction using self-developed aortic valve plasty system in aortic valve disease. *Interact Cardiovasc Thorac Surg* 2011;**12**:550–3.
8. Ozaki S, Kawase I, Yamashita H, Uchida S, Takatoh M, Kiyohara N. Midterm outcomes after aortic valve neocuspidization with glutaraldehyde-treated autologous pericardium. *J Thorac Cardiovasc Surg* 2018;**155**:2379–87.
9. Polito A, Albanese SB, Cetrano E, Forcina S, Cicenia M, Rinelli G *et al.* Aortic valve neocuspidalization may be a viable alternative to ross operation in pediatric patients. *Pediatr Cardiol* 2021;33394106
10. Wiggins LM, Mimic B, Issitt R, Ilic S, Bonello B, Marek J *et al.* The utility of aortic valve leaflet reconstruction techniques in children and young adults. *J Thorac Cardiovasc Surg* 2020; **159**:2369–78.
11. Baird CW, Sefton B, Chávez M, Sleeper LA, Marx GR, del Nido PJ. Congenital aortic and truncal valve reconstruction utilizing the Ozaki technique: short-term clinical results. *J Thorac Cardiovasc Surg* 2020; doi:10.1016/j.jtcvs. 2020.01.087.
12. Bissell MM, Hess AT, Biasiolli L, Glaze SJ, Loudon M, Pitcher A *et al.* Aortic dilation in bicuspid aortic valve disease: flow pattern is a major contributor and differs with valve fusion type. *Circ Cardiovasc Imaging* 2013;**6**:499–507.
13. Meierhofer C, Schneider EP, Lyko C, Hutter A, Martinoff S, Markl M *et al.* Wall shear stress and flow patterns in the ascending aorta in patients with bicuspid aortic valves differ significantly from tricuspid aortic valves: a prospective study. *Eur Heart J Cardiovasc Imaging* 2013;**14**:797–804.
14. Kelm M, Goubergrits L, Fernandes JF, Biocca L, Pongiglione G, Muthurangu V *et al.* MRI as a tool for non-invasive vascular profiling: a pilot study in patients with aortic coarctation. *Expert Rev Med Devices* 2016;**13**.
15. Guzzardi DG, Barker AJ, Van Ooij P, Malaisrie SC, Puthumana JJ, Belke DD *et al.* Valve-related hemodynamics mediate human bicuspid aortopathy: insights from wall shear stress mapping. *J Am Coll Cardiol* 2015;**66**:892–900.
16. Bissell MM, Loudon M, Hess AT, Stoll V, Orchard E, Neubauer S *et al.* Differential flow improvements after valve replacements in bicuspid aortic valve disease: a cardiovascular magnetic resonance assessment. *J Cardiovasc Magn Reson* 2018;**20**:10.
17. Polito A, Albanese SB, Cetrano E, Cicenia M, Rinelli G, Carotti A. Aortic valve neocuspidalization in pediatric patients with isolated aortic valve disease: early experience. *Interact Cardiovasc Thorac Surg* 2021;**32**:111–117; doi: 10.1093/icvts/ivaa237.
18. Dyverfeldt P, Bissell M, Barker AJ, Bolger AF, Carlhäll C-J, Ebbers T *et al.* 4D flow cardiovascular magnetic resonance consensus statement. *J Cardiovasc Magn Reson* 2015;**17**:72.
19. Hope MD, Hope TA, Crook SES, Ordovas KG, Urbania TH, Alley MT *et al.* 4D flow CMR in assessment of valve-related ascending aortic disease. *JACC Cardiovasc Imaging* 2011;**4**:781–7.
20. Von Knobelsdorff-Brenkenhoff F, Trauzeddel RF, Barker AJ, Gruettner H, Markl M, Schulz-Menger J. Blood flow characteristics in the ascending aorta after aortic valve replacement—a pilot study using 4D-flow MRI. *Int J Cardiol* 2014;**170**:426–33.
21. Zoghbi WA, Adams D, Bonow RO, Enriquez-Sarano M, Foster E, Grayburn PA *et al.* Recommendations for noninvasive evaluation of native valvular regurgitation: a report from the American Society of Echocardiography Developed in Collaboration with the Society for Cardiovascular Magnetic Resonance. *J Am Soc Echocardiogr* 2017;**30**:303–71.
22. Brancaccio G, Polito A, Hoxha S, Gandolfo F, Giannico S, Amodeo A *et al.* The Ross procedure in patients aged less than 18 years: the midterm results. *J Thorac Cardiovasc Surg* 2014;**147**:383–8.
23. Luciani GB, Lucchese G, Carotti A, Brancaccio G, Abbruzzese P, Caianiello G *et al.* Two decades of experience with the Ross operation in neonates, infants and children from the Italian Paediatric Ross Registry. *Heart* 2014;**100**:1954–9.
24. Hörer J, Kasnar-Samprec J, Charitos E, Stierle U, Bogers AJJC, Hemmer W *et al.* Patient age at the Ross operation in children influences aortic root dimensions and aortic regurgitation. *World J Pediatr Congenit Heart Surg* 2013;**4**:245–52.
25. Chivers SC, Pavy C, Vaja R, Quarto C, Ghez O, Daubeney PEF. The Ozaki procedure with CardioCel patch for children and young adults with aortic valve disease: preliminary experience—a word of caution. *World J Pediatr Congenit Heart Surg* 2019;**10**:724–30.
26. Davies PF. Hemodynamic shear stress and the endothelium in cardiovascular pathophysiology. *Nat Rev Cardiol* 2009;**6**:16–26.
27. Callaghan FM, Grieve SM. Normal patterns of thoracic aortic wall shear stress measured using four-dimensional flow MRI in a large population. *Am J Physiol Hear Circ Physiol* 2018;**315**:1174–81.
28. Callaghan FM, Kozor R, Sherrah AG, Vallely M, Celermajer D, Figtree GA *et al.* Use of multi-velocity encoding 4D flow MRI to improve quantification of flow patterns in the aorta. *J Magn Reson Imaging* 2016;**43**:352–63.
29. Rose MJ, Rigsby CK, Berhane H, Bollache E, Jarvis K, Barker AJ *et al.* 4-D flow MRI aortic 3-D hemodynamics and wall shear stress remain stable over short-term follow-up in pediatric and young adult patients with bicuspid aortic valve. *Pediatr Radiol* 2019;**49**:57–67.
30. Van Ooij P, Powell A L, Potters W V, Carr J C, Markl M, Barker A A J.Reproducibility and interobserver variability of systolic blood flow velocity and 3D wall shear stress derived from 4D flow MRI in the healthy aorta. J Magn Reson Imaging 2016;**43**:236–48. 10.1002/jmri.24959